

Ultrasound Added Additive Manufacturing for Metals and Composites: Process and Control



Sachin Kumar and Brij Kishor

1 Introduction

The ultrasonic vibrations find their applications in various conventional manufacturing processes to cope with their multiple shortcomings [25]. For example, ultrasonic-assisted machining, forming, welding, friction stir welding are well-established and niche techniques [8, 24, 28, 32, 33, 39]. The ultrasonic vibrations denote the sound waves beyond human hearing range and correspond to the frequency range close to 20 kHz [21, 25]. Based on the frequency ranges, the categorization of sound waves and their corresponding applications has been shown in Fig. 1. The sound waves in the ultrasonic range can be used for various medical and manufacturing processes. Depending on the intrinsic elastic properties and densities, ultrasonic waves can travel with different velocities in different types of mediums [35]. The ultrasonic waves initiate mechanical vibrations into the medium and provoke molecular displacement at the micron level. In the form of the wave, ultrasonic vibrations can travel from one medium to another. However, their movement chiefly depends on ultrasonic vibration frequency, amplitude, and medium of wave propagation, etc. [35]. The ultrasound addition in additive manufacturing processes (AM) process [68] is quite new and has gained serious attention from various researchers across the globe.

The Ultrasonic Additive Manufacturing (UAM) is a solid-state manufacturing process, invented and patented by Dr. White [74], and commercially marketed by Fabrisonic LLC, USA. The UAM is based on the principle of bonding the thin metal

S. Kumar (✉)

MOE Key Lab for Liquid-Solid Structure Evolution and Materials Processing, Institute of Materials Joining, Shandong University, Jinan 250061, People's Republic of China

B. Kishor

Department of Materials Science and Engineering, National Institute of Technology, Hamirpur (H.P.), India

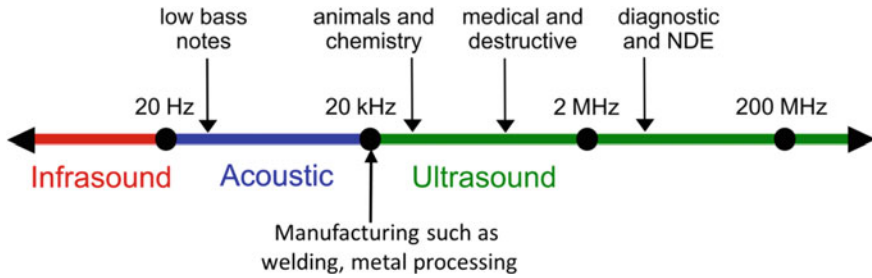


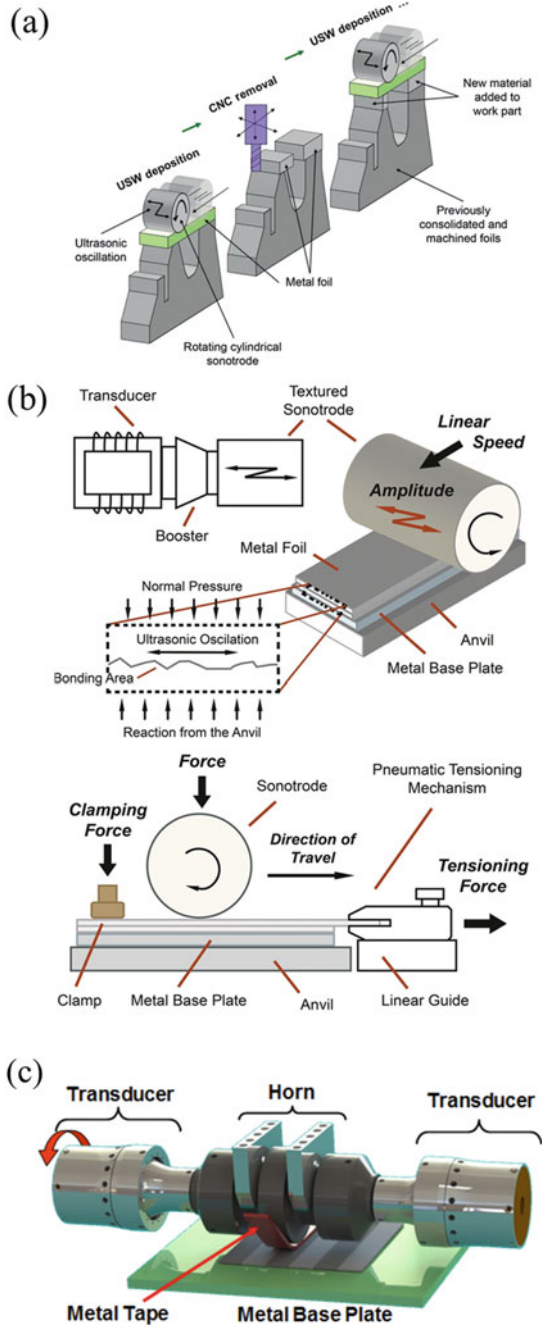
Fig. 1 Wave frequencies with their typical range and applications ('Ultrasound')

foils together sequentially using a similar concept as the ultrasonic metal welding process [14]. The bond formation is done layer by layer on Computer Numerical Control (CNC) machining to cut unwanted material and replicate the desired shape and size (Fig. 2). Therefore UAM can be referred to as the hybrid manufacturing process involving metal addition and subtraction. Typically a UAM process consists of a sequential arrangement of an ultrasonic generator, transducer, booster, and horn/sonotrode. The detailed description of these components has already been given elsewhere hence omitted in the present context [12, 25].

The UAM process involves the generation and transfer of ultrasonic energy from the output end of the transducer to a metallic work-piece via specially designed ultrasonic horn/sonotrode in the form of to and fro oscillations. The simultaneous interaction of normal compressive load with the ultrasonic oscillation permits localized heating of the material intended to work in the close vicinity of contact area, allowing the inter-laminar material flow in that region. It is important to note that the localized rise in material temperature in this process is considerably less to the melting point temperature of respective metal (approximately 50% of the melting temperature). Such a situation permits the metals to have solid-state interaction across their adjoining regions in order to form a bond [37, 69].

This additive buildup by ultrasound-assisted solid-state joining followed by simultaneous selective subtraction can consequent many key manufacturing features such as joining of mechanically and thermally dissimilar materials even of different thicknesses, retaining the original microstructure and grain orientation of parent metals even after joining, safe inclusion/embedding of functional components such as electronic switches or sensors in between the metal foils. The material bonding in the UAM process primarily depends on material processing and ultrasonic parameters such as horn oscillation, the compressive force exerted on the work-piece, and the travel speed of the horn. The selection of optimum values of all these parameters is vital as any deviation may severely degrade the bond quality [22]. In a similar context, Hopkins et al. [18] and Wolcott et al. [76] recognized the horn amplitude and travel speed as the most influential parameters to achieve high strength bonds.

Fig. 2 a–c Schematic diagram of UAM process [3, 12, 61] ('Printing Metal 3D Objects Using Sounds')



2 Metallic Bonding of Dissimilar Materials

One of the most promising features of the UAM process is its capability to join dissimilar materials under solid-state conditions even if there is a nominal gap in their melting point temperature. This promising feature makes it stand out among various other additive and traditional manufacturing techniques. In UAM, the inherent mechanical and metallurgical properties of base metals remain intact due to the absence of their melting. Thus makes it applicable for high-strength aerospace aluminum alloys that are not susceptible to be thermally welded without any significant material property loss. The solid-state nature permits the reduction or elimination of brittle intermetallics (IMCs), whose massive formation has been reported in conventional processes. It is essential to mention that brittle IMCs phases attract lateral cracking and therefore severely degrade the structure’s joint quality [48, 80]. Several metal combinations that have been processed with ultrasonic welding (USW) may not have been attempted in UAM and therefore can be the hotspot for future research. Figure 3 shows some known metal combinations that are available for USM and UAM processes.

Furthermore, by adding different materials of different thicknesses in a predefined manner, UAM can produce functionally graded laminates with great ease that can be quite cumbersome by other conventional manufacturing methods. The metallic foils can be placed alternatively in layers and welded into a layered structure to form multi-material laminates (Fig. 4). Via placing different materials in different thicknesses, the mechanical properties of the structure can be carefully controlled. For example, Solidica Inc. has used this technique to produce aluminum and titanium in varying ratios to develop armor applications’ layered structure.

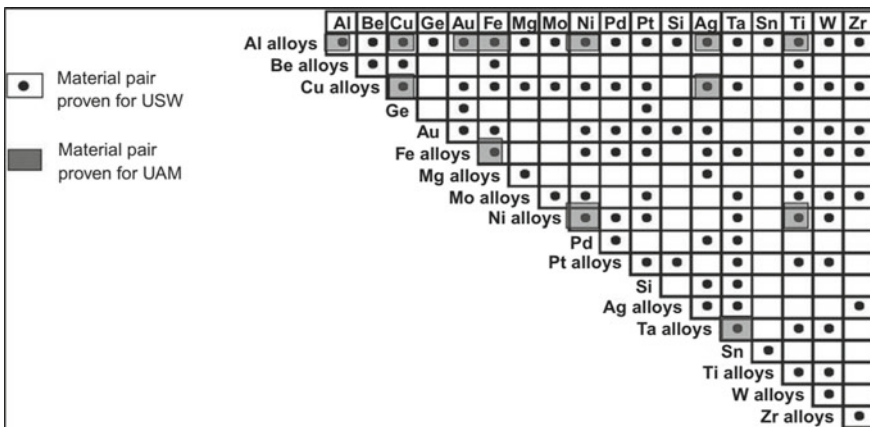


Fig. 3 Material combinations applicable for USM and UAM [12, 19], Image courtesy of the American Welding Society

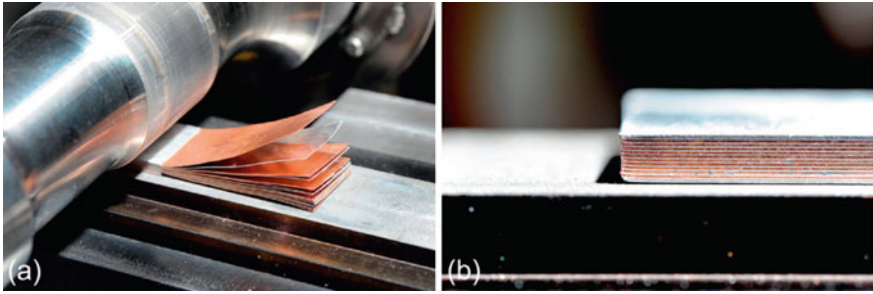
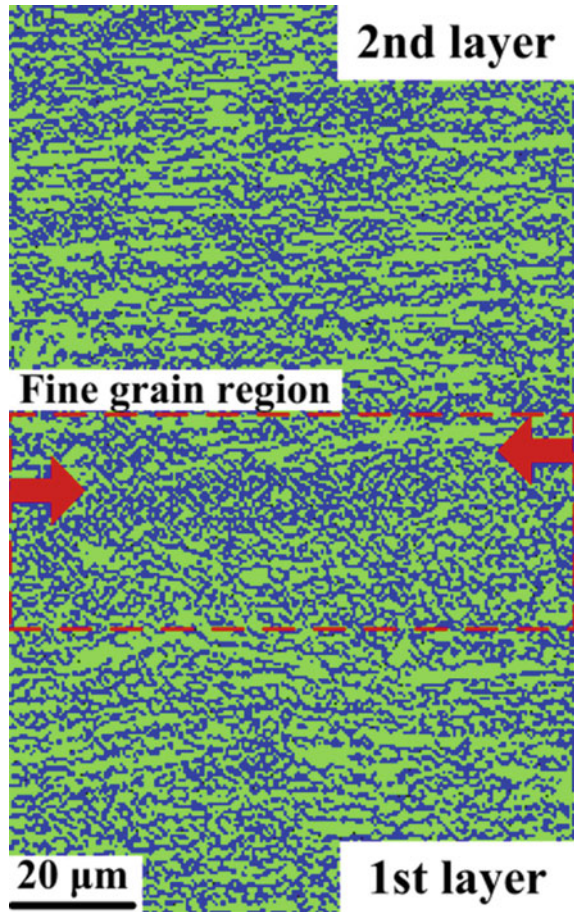


Fig. 4 a, b UAM dissimilar materials bonding for alternative layers of Al and Cu foils [12], Image courtesy of Loughborough Universities Additive Manufacturing Research Group

The UAM, being an advanced manufacturing technique, can support the manufacturing of complex and challenging to produce shapes with high precision and excellent surface finish. It can be due to the absence of the melting of the respective metals that minimizes the dimensional ambiguities that are usually observed in shrinkages, residual stresses, and distortion of metal parts [58]. The UAM is also effective in producing various manufacturing components of several materials, such as metal matrix composites, parts with embedded wirings, sensors etc., [50]. Frictional heat produced in this process can be regarded as the major source of material bonding. It can be approximately two times that of heat obtained from the plastic deformation of the material [70]. Besides, the ultrasonic addition can add the shear scrubbing that can break up the oxide layer formed on material surfaces. It permits the virgin material surface to interact and bond between the layers [5]. The foils experience intense acoustically induced softening due to ultrasonic vibrations, which affects the material lattice and imparts the plastic deformation [34, 79]. The welds characteristic and their formation mechanism during the ultrasonic-assisted process have been documented by Shimizu et al. [64] by analyzing their microstructural evolution. They observed that acoustic assistance could produce refined and equiaxed grains in the stirred zone (SZ) due to the intense grain refinement and recrystallization occurred by sequential heating and shear deformation. The grain refinement across the joint regions for the first and second layers of the aluminum alloy parts can be seen in Fig. 5 [64]. Dehoff and Babu [6], Mariani and Ghassemieh [45] have analyzed the microstructural evolution during ultrasonic assistance to analyze the possible bonding characteristics during the solidification and recrystallization stage.

To explain the importance and role of ultrasonic vibrations on the bonding mechanism during the UAM process, the microstructural analysis has been investigated by several researchers. For example, Pal and Stucker [52] proposed a finite element model to determine the microstructural evolution in case of the ultrasonic-assisted process by adopting dislocation-density-based crystal plasticity theory. Their work focused on the quasi-static formulation of large plastic deformation, material model based on non-local dislocation density, and process boundary conditions. They concluded that before and after processing, the grain size was reduced to 1.2 μm

Fig. 5 Fine grains around the interface regions between the first and second layers in the aluminum alloy parts fabricated with ultrasonic addition [49, 64]



from the average value of 13 μm . The simulated results were compared with experimental data and found in good agreement. In the UAM process, the amplitude of ultrasonic vibrations plays an important role in the process parameters' effectiveness. They affect the material flow and plasticity at the region of contact [70]. It has been reported that the parts fabricated with high ultrasonic amplitude can yield better tensile properties that almost approach the value of bulk materials [11]. Apart from that, under the influence of large amplitudes, defects are suppressed greatly, and better bonding is experienced in the fabricated aluminum parts as shown in Fig. 6 [67]. It could be because the large amplitude might induce a significant portion of linear weld density with a more compact foil layer.

It is important to note that higher ultrasonic vibration amplitude induces severe plastic deformation with enhanced material plastic flow that suppresses the defects and improves the bonding [57]. The ultrasonic vibration induced consolidation is also beneficial to produce the metal matrix composites. Their bond strength can also

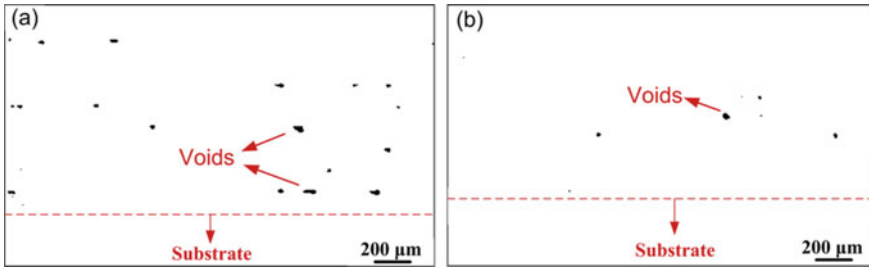


Fig. 6 Optical images of Al alloy parts produced by ultrasonic consolidation process **a** at lower ultrasonic amplitude and **b** at higher ultrasonic amplitude [49, 67]

be analyzed by interface failure which depicts that a higher value of composite length could minimize composite failure probability [16]. To have better knowhow of the interfacial strength, Hehr and Dapino [17] analyzed the interface quality via a single fiber pullout test. They concluded that the bonding was dependent on the fiber surface finish.

Apart from UAM, friction stir welding process (FSW) [2, 20, 55, 66, 77] added with ultrasonic vibration has been found utilizing their virtue to promote the material flow and enhance the bonding of metals across their joining regions [26, 72]. To analyze the virtues of ultrasonic vibrations in the material joining process, recently Kumar et al. [27] have designed and developed an ultrasonic vibration-assisted friction stir welding (UVaFSW) system (Fig. 7) similar to Park [54] and Kumar [24]. This

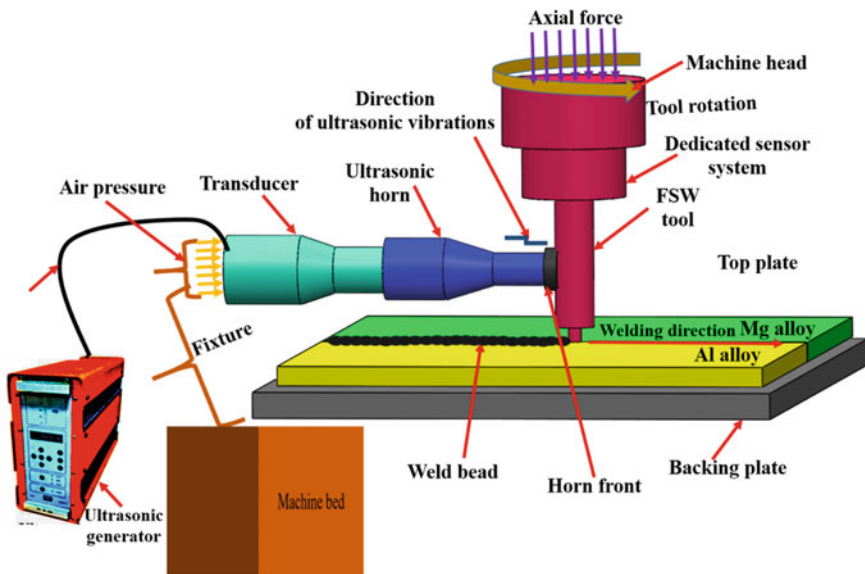


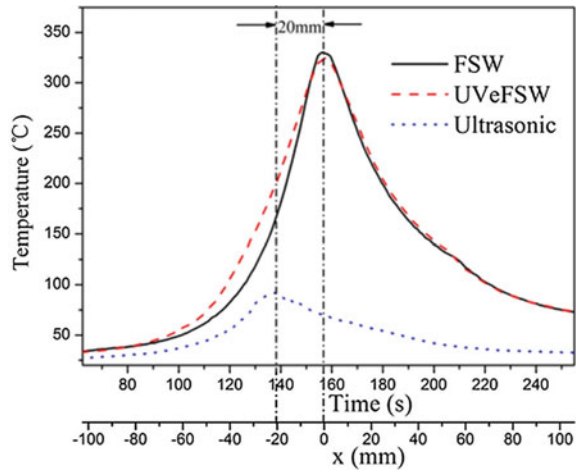
Fig. 7 Schematic of ultrasonic assisted friction stir welding system [29]

ultrasonic vibration is aimed to transfer the acoustic energy in the SZ via welding tool. The aforesaid UVaFSW system comprises a specially designed ultrasonic horn, front attachments, and a welding tool to safeguard the system and safely transfer the ultrasonic energy at the required region. Roller bearings are added to smoothen the process of ultrasonic vibrations from the stationary horn to the rotating FSW tool. In order to gather further details on UVaFSW system, readers can refer the author's previous work Kumar et al. [27, 28, 30], Kumar and Wu [33] have reported major benefits of ultrasonic energy on the joint quality. Additionally, the axial force, torque, and power requirements can also be significantly reduced, which can help to reduce the tool wear and enhance its life. An enhanced material plasticization of the SZ under intense acoustic softening can be reasoned for better joint quality. The ultrasonic addition also favors to reduce the flow stresses and improve the material flow under the vicinity of the ultrasonic vibration zone.

Park et al. [53] enforced the ultrasonic vibrations with the FSW process on the welding tool along the horizontal direction. They found a substantial drop in axial force and marginal rise in weld properties. In a similar ultrasonic addition, Kumar [24] claimed a notable reduction in axial downward force and significant improvement in weldment properties during FSW of Al alloys. However, the frequent failures of horn attachments are evident during experimentation, which restricts their results' reproducibility. Ruilin et al. [60] added a similar mode of ultrasonic energy and reported that the impact of acoustic addition on temperature fields in the FSW process is less effective at lower welding speeds. It can be attributable to additional heat addition due to ultrasonic vibrations. At lower rotation speeds, the peak temperature was identical for both the processes, while a reduction in maximum temperature is higher in the case of FSW than the UVaFSW for higher welding speeds. Ma et al. [44] reported that the weld properties were enhanced during ultrasonic addition in FSW when acoustic intensity was 50%. Amini and Amiri [1] also found a notable reduction in FSW axial force during ultrasonic addition, which could be due to improved weld penetration [1, 24]. Their analysis emphasized that an increase in welding speed in the FSW process could increase the axial force marginally, while the same could be reduced with an increase in rotation speed. The ultrasonic addition could cause better material stirring and enhanced plastic flow. The weld strength and elongation are also improved by ~10% during ultrasonic addition in the FSW process.

Liu et al. [40] designed and developed a novel ultrasonic vibration enhanced FSW (UveFSW) system via simple linkages, where ultrasonic energy is imparted on the work-piece just ahead of the welding tool by the sonotrode inclined at ~40°. They obtained better material flow and improved weld properties using such kind of UveFSW system. Liu et al. [41] discovered that better joint quality in the UveFSW process is due to intensive material plasticization and reduced HAZ. The weld microstructures analysis reported that the ultrasonic addition could improve the material mixing, deformation in the SZ, and enlarge the thermo-mechanically affected zone (TMAZ). The weld strength was increased marginally due to the improved material flow. Liu et al. [40] analyzed the material flow during the UveFSW of Al alloy by utilizing a marker insert and sudden stop-action method. During the UveFSW, they noticed intense material plasticization and improved material flow rate. It could

Fig. 8 Temperature variation for FSW and UVeFSW process [81]



be due to supplementary material plasticization under ultrasonic addition. Shi et al. [63] modeled the quasi-steady state of the UVeFSW process. Their model predicted that the better material flow could be due to the ultrasonically influenced stirring and flow stress reduction. The aforesaid ultrasonic-assisted model Shi et al. [63] also discovered that the UVeFSW had minor effects on the overall heat addition and temperature field during the welding. Zhong et al. [81] obtained a notable reduction in tool torque and axial load with ultrasonic addition in FSW process. They also compared the temperature field without ultrasonic addition (FSW) and UVeFSW as shown in Fig. 8. During the weld advancement, the temperature rise in the UVeFSW is reported higher compared to the FSW process. The maximum temperature difference is between the two processes is reported ~40 °C, which occurred 20 s before the peak value. This signifies that ultrasonic vibration heat up the welding material that causes it to experience higher temperature for a considerable time [81].

The weld macrographs at different process parameters for both FSW and UVeFSW processes are shown in Fig. 9. The boundary of pin affected zone of SZ in the case of UVeFSW is surprisingly enlarged than that of FSW. The interface between the SZ and TMAZ across the AS is also smoother for UVeFSW joints.

The FSW joints are found to have defects in the lower section of SZ because of inadequate heat input and poor material mixing. On the contrary, most of the UVeFSW joints are defect-free in SZ. It is attributable to better material mixing and improved material flow [26, 81]. Liu and Wu [42] discovered that the tunnel defects could be eliminated completely with ultrasonic induction in the FSW process. For the FSW and UVeFSW processes, Padhy et al. performed microstructure evolution across the SZ of Al alloy using the advanced microstructure techniques [51]. Their outcomes have shown that acoustic addition has significantly refined the grains and sub-grain formation at the SZ. Finally, ultrasonic addition in the FSW process has been proven robust, beneficial, and superior in context to the process efficacy and joint characteristics than that of the conventional FSW [26]. The acoustic assistance can

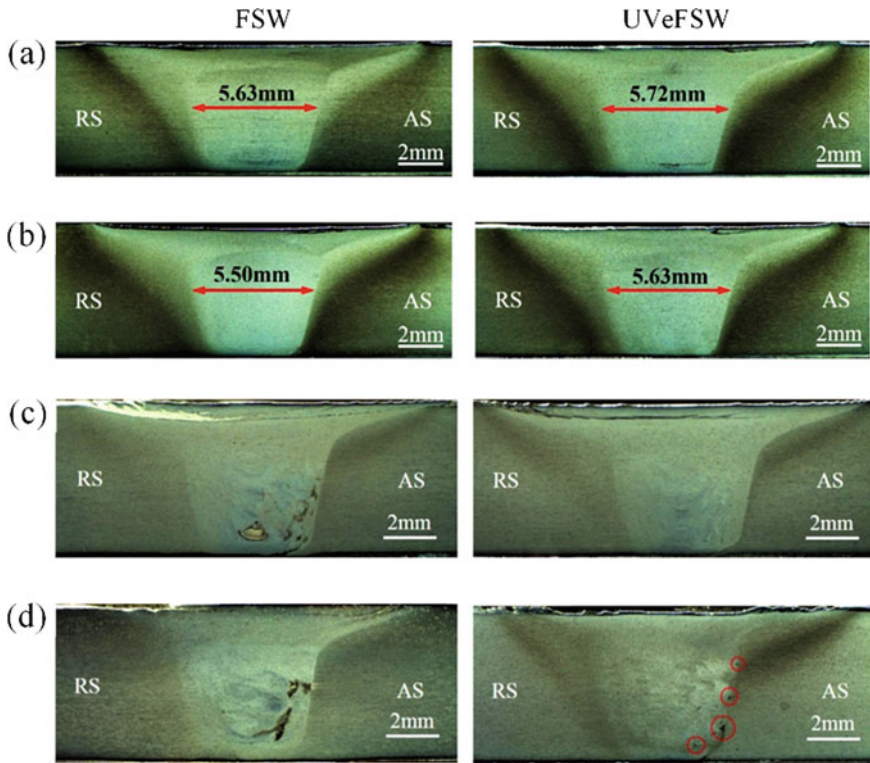


Fig. 9 The optical images of FSW and UVeFSW joints of AA2024-T3 alloy at **a** 200 rpm, 110 mm/min, plunge depth = 0.1 mm, and **b** 400 rpm, 330 mm/min [81]

significantly improve the weld properties and material flow, enlarge process window, suppressed the weld anomalies, and improve the weld quality and microstructure.

Tarasov et al. [71] developed another method to apply for acoustic assistance in front of the welding tool via the backing plate for FSW of Al alloy. They narrated that acoustic energy helped to suppress the recrystallized grain size in SZ at weldment. It is suggested ultrasonication may retard the GP ripening due to the dynamic stabilization of the solid solution. Additionally, the ultrasonic energy might have smoothed the strain-induced dissolution of earlier thought insoluble coarse Al–Cu–Fe–Mn particles. Lv et al. experimented on the FSW of dissimilar Al/Mg alloys by applying ultrasonic vibration system at an angle to the welding tool. They obtained a notable rise in the weld quality and claimed the IMCs phases disappearance across the interface [43]. Besides, they added that with the addition of acoustic assistance, IMCs (Al_3Mg_2 (layer 1) + $\text{Al}_{12}\text{Mg}_{17}$ (layer 2)) of overall thickness $\sim 3.5 \mu\text{m}$ gradually became a monolayer (Al_3Mg_2) of overall thickness $\sim 2.5 \mu\text{m}$. Kumar et al. [29] performed the scanning electron microscopic (SEM) analysis of the SZ to determine the advantages of ultrasonic energy on the FSW process (Fig. 10). The SZ of both Al and Mg alloys resembles significantly refined and smaller grains as compared to

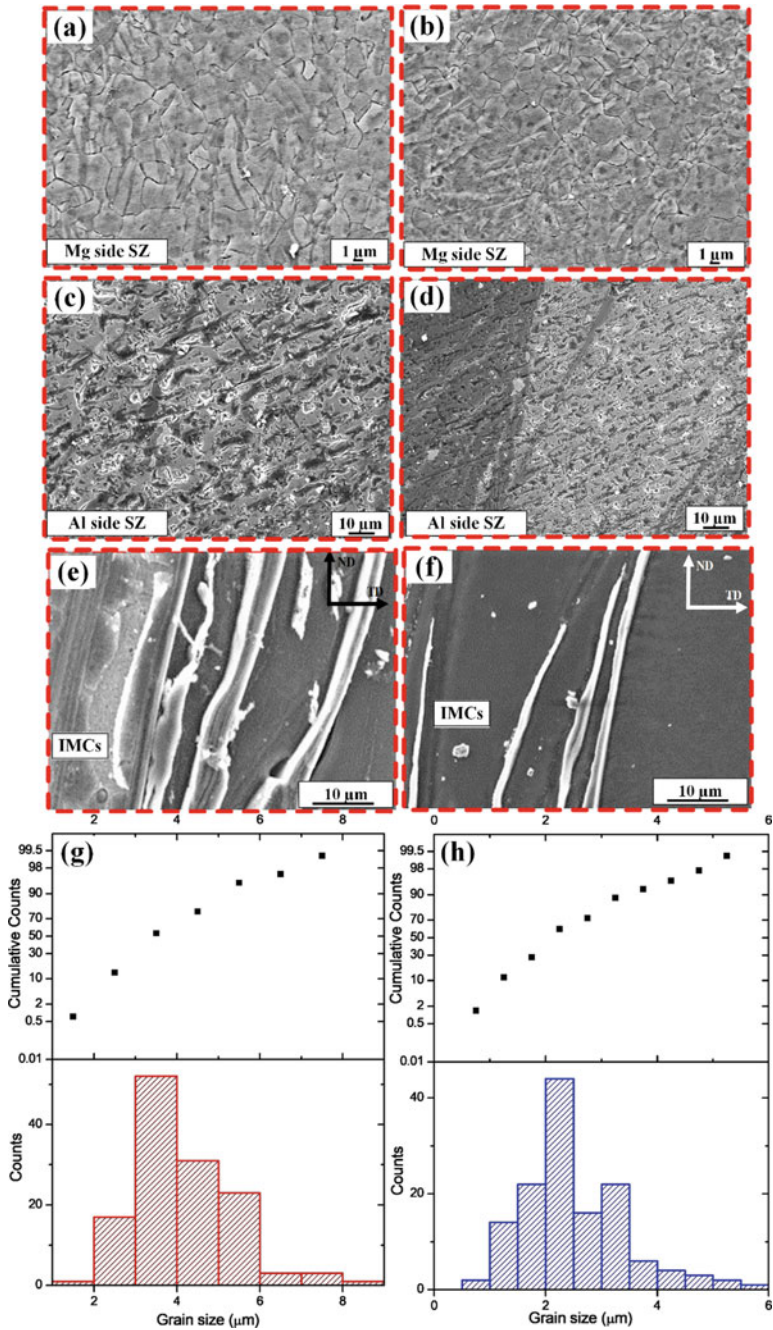


Fig. 10 High magnification images of FSW and UVaFSW joints across the SZ **a, b** Mg Side **c, d** Al side and **e, f** IMCs region **g, h** the grain size analysis for Mg side [29]

the base metals (Fig. 10). It is also observed that the grains are recrystallized and finer for the ultrasonic welds at Mg side compared to the conventional FSW joints. The grain analysis of the SZ of the Mg side shows average grain size of ~ 2.5 and $4.16 \mu\text{m}$ for ultrasonic and non-ultrasonic welds respectively (Fig. 10a, b, g, h). It implies that acoustic energy is helpful to refine and reduce the grain size. Similarly the grain analysis of SZ region also shows comparatively fine and equiaxed grains for the ultrasonic joints. This region also advocates the intense intermixing of various substrates in a complex manner because of Al alloys' intense material plasticization compared to the Mg alloy [36].

The formation of the dendrite structure in the Al alloys' weld zone in the case of the FSW process is quite common that may be due to constitutional liquation. The phenomenon of constitutional liquation for the FSW process has been reported previously in different studies [4, 7]. During the FSW of Al/ZrB₂ Dinaharan and Murugan [7] have quoted that the constitutional super cooling can originate the dendritic structure during the solidification process. Similarly, in case of dissimilar FSW of Al and Mg alloys, Firouzdor and Kou [9] have also reported dendrites formation of Al₃Mg₂ and Al₁₂Mg₁₇. The high magnification images of the IMCs region depicts heavy lumps of intermixed substrates in SZ-TMAZ (Fig. 10e) that may resemble the IMCs of Al and Mg. The origin of heavy lumps of IMCs can be ascribed to the intense intermixing of Al and Mg substrates followed by flow of Al lamellae across the advancing side (AS) and material stirring across shoulder and pin region. The formation of discrete particles is primarily controlled by the SZ region's heat input and formed because of the controlled by inter-diffusion or eutectic transformation [43]. The nature of IMCs formation largely depends on the concentration of Al and Mg substrates [30]. The region where Al concentration dominates attracts Al₃Mg₂ while that of Mg dominated region probably have Al₁₂Mg₁₇. The same can be ascribed from the binary phase diagram of Al and Mg alloys [10].

3 Object Embedment

Further application of ultrasonic addition has been experienced by digging out the possibility of embed fibers, electronic circuits, or structures in the metal matrix. Heavy material flow in presence at low temperature permits safe embedment without any harm to embedding material. The embedment process follows the binding of metal foil material with the base metal by the horn/sonotrode. The foil fibers or electronic circuit are added on this, and the second layer of foil is then placed on the top of the embed object followed by sonotrode contact to the sample to bond it with the previous layer. Under the influence of the acoustic plastic behavior of metal foil in contact with the horn pressure and oscillation, the foil is plastically deformed around the embed material. It makes contact with the previous foil layer, thus forming a solid-state bond (Fig. 11).

Following the unique feature of UAM, the embedment of various materials has endeavored in previous literature. Li et al. [38] have attempted the embedment of

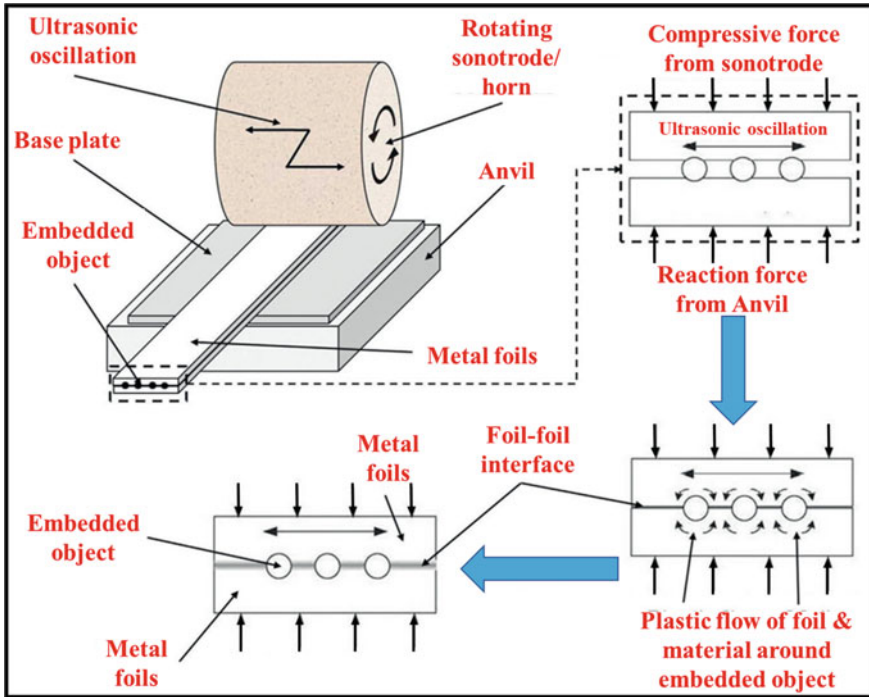


Fig. 11 a, b The schematic process of object embedding via UAM process [12, 13]

printed electronic pathways in between the Al foils interface. Similarly, Robinson et al. [59] and Siggard et al. [65] have successfully added the pre-packed electronic circuit system in the metal grooves created by the CNC machine. Kong and Soar [23] have carried out the embedding of polymer-based coated and uncoated optical fibers in the Al matrix. In a similar attempt, Monaghan et al. [46] and Mou et al. [47] have also successfully implemented metal-coated optical fibers and Bragg fibers in their research findings. The UAM technique has been advanced by embedding the shape memory alloy fibers in the Al matrix and investigated by Friel and Harris [13] and Hahnlen and Dapino [16]. Their findings have reported appreciable functionality of embedded components and excellent bond strength of adjoining layers. Hence UAM can be considered as one of the most appropriate techniques to develop the embedded structures.

At several places, the UAM is also referred to as a “bond-then-form” technique [15]. It is because, after UAM bonding, subsequent CNC machining is required to add up to cast the anticipated form to the bonded metallic foils. This process is completed in a number of steps followed by layer bonding, it’s machining, layer bonding on previously formed part followed by further machining until the required 3D shape is not attained. Similarly, in the “form-then-bond” approach, the required 3D shape is cast in each joined layer (via suitable machining process such as laser

machining) before its binding to the earlier formed part. This method can allow to form the structures to have inner geometry and channels that are quite cumbersome to produce via the “bond-then form technique” [15]. This process has been proven beneficial in developing functional ceramic parts and microfluidic systems via the Computer Aided Manufacturing process ([3], Cawley et al.)

Bournias-Varotsis et al. [3] have analyzed the ultrasonic welding of aluminum foils followed by the geometric machining prior to the commencement of the bonding (Fig. 12). These pre-machined geometries can facilitate to keep the foil in layer by layer in a predefined sequence to host any electronic or fragile components in a required groove, gap, or pocket. For the UAM process, the deformation mechanics of the aluminum foils could be studied and a model was proposed that could facilitate estimation of the final location, shape and size, and tolerances of pre-machined features for a defined combination of process parameters. The proposed model was tested by hosting an electronic component before its encapsulation in a predesigned cavity. In the present example (Fig. 12), the embedment of an electronics item is made however the same can be applied for the fabrication of microfluidic or thermal management devices also. Here, the aluminum foil is machined before being bonded via the UAM process. The cavities and channels are formed layer by layer to form features to host the electronic circuitry. In the process, for the cross-sectioned sample,

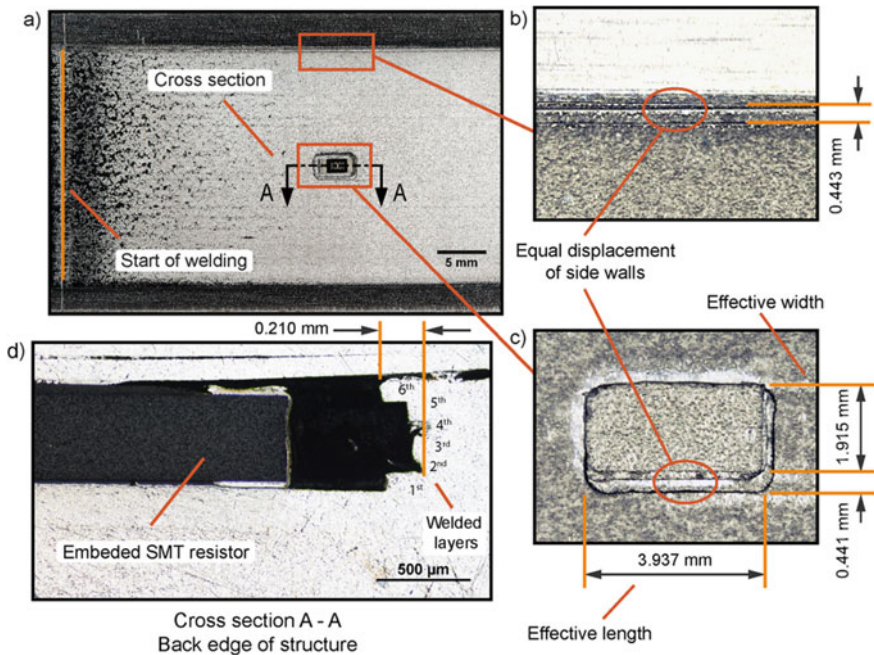


Fig. 12 Representation of multi-layer structure. **a** Top view before encapsulation. **b** Close up of the top edge of the bonded foils. **c** Fabricated structure. **d** Cross-section of the back edge of the structure after encapsulation [3]

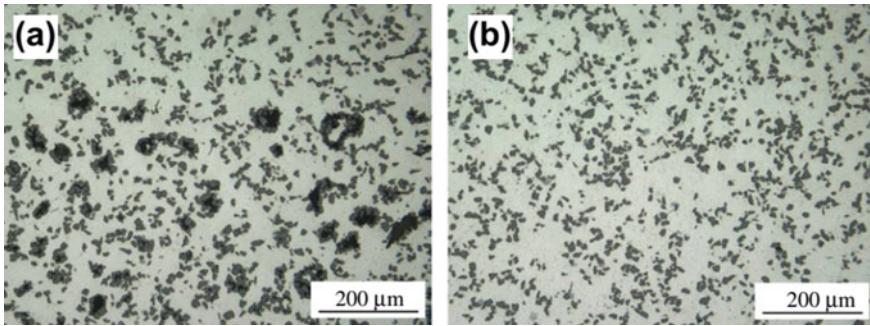


Fig. 13 The microstructure profile of reinforced filler metals **a** via stir casting and **b** via ultrasonic assistance [78]

any visible destruction in the resistor was seen. It is important to note that the effective measured width was found smaller than that of the predicted one in this case. It may be due to human error incurred while foil placement and its alignment before the welding process's commencement.

The UAM has been proven beneficial to fabricate a wide variety of industrially applicable composites. For example, the addition of silicon carbide particulate into the Al matrix may offer several benefits. Wielage et al. [75] performed ultrasonic-assisted soldering of $\text{Al}_2\text{O}_3/\text{6061}$ metal matrix composites by adding SiC reinforced and Sn-based solders. They reported significantly homogenized reinforced joints of SiC with an appreciable improvement in joint strength than that of a non-reinforced joint. Yan et al. [78] attempted SiC reinforced and Zn-based filler to fabricate the $\text{SiC}_p/\text{A356}$ composites with the aid of ultrasonic vibrations. During the joining, the ultrasonic assistance has been proven beneficial to disperse the agglomerates and eliminated the possibility of SiC coagulation. A complete absence of voids and enhanced intermixing of particles in the metal matrix have been observed that may be due to the ultrasonic vibration effects.

The high-resolution microstructure images of $\text{SiC}_p/\text{Zn-Al}$ filler metals have been shown in Fig. 13. Adequate intermixing of stir cast filler with the SiC substrates is observed at subsequent intervals. However, noticeable particle segregation and voids gaps can be seen in the metal matrix (Fig. 13a). With ultrasonic assistance, the localized particle segregation has been considerably reduced while voids' intensity is trimmed, replicating the homogenized mixture of the metal matrix (Fig. 13b).

4 Conclusion and Future Perspective

From the aforesaid discussions, it has been observed that a significant amount of effort has been added to utilize the benefits of ultrasonic vibrations in the form of the ultrasound-assisted manufacturing process. The effect of ultrasonic assistance in

various manufacturing processes has been dealt with in detail and their processing mechanism is discussed to grasp the fundamental concepts. The ultrasound assistance can suppress the defect frequency and improves the material flow that in turn enhance the part quality. With the addition of ultrasound, the surface characteristics and dimensional accuracy can be enhanced than that of the conventional manufacturing processes (without ultrasound). The acoustic assistance can also reduce the frictional contacts between the machine parts, hence the force required to do the required job can also be reduced. Among these astonishing properties, better arranged high compact density and good surface quality make the ultrasound-assisted as a unique technique in the manufacturing domain. In ultrasonic-assisted compaction, the vibration energy breaks the oxide layer, softens the localized region of contact and results in strong bonding in the case of 3D structures. In case of UAM, the ultrasonic addition can produce non-linear effects for example, acoustic streaming and cavitation. All this can alter the magnitude of heat and mass transfer and thereby the grain refinement and crystal growth. Apart from that, several other special effects such as enhanced stirring, better material mixing and crystal dispersion cum nucleation can be seen in case of melting materials. A better degree of material homogenization by liquid agitation, enhanced particles distribution, and suppressed frequency of porosity and cracks in presence of ultrasonic vibration can be seen from the results reported. As a result the manufactured parts have better quality and precise control in their dimensional accuracy. This short literature review can assist the readers to grasp the basic concepts and application domains of the ultrasonic energy in manufacturing context. It can also be helpful to advance better and effective systems to impart ultrasonic vibrations into the manufactured zone.

References

1. Amini S, Amiri M (2014) Study of ultrasonic vibrations effect on friction stir welding. *Int J Adv Manuf* 73(1–4):127–135
2. Bansal A, Singla AK, Dwivedi V, Goyal DK, Singla J, Gupta MK, Krolczyk GM (2020) Influence of cryogenic treatment on mechanical performance of friction stir Al–Zn–Cu alloy weldments. *J Manuf Process* 56:43–53
3. Bournias-Varotsis A, Friel RJ, Harris RA, Engström DS (2018) Ultrasonic Additive manufacturing as a form-then-bond process for embedding electronic circuitry into a metal matrix. *J Manuf Process* 32:664–675
4. Chen YC, Nakata K (2008) Friction stir lap joining aluminum and magnesium alloys. *Scripta Mater* 58(6):433–436
5. Chua CK, Leong KF (2014). 3D printing and additive manufacturing: principles and applications (with companion media pack)—Fourth edition of rapid prototyping, 3d printing and additive manufacturing: principles and applications (with companion media pack)—Fourth edition of rapid prototyping
6. Dehoff R, Babu S (2010) Characterization of interfacial microstructures in 3003 aluminum alloy blocks fabricated by ultrasonic additive manufacturing. *Acta Mater* 58:4305–4315
7. Dinaharan I, Murugan N (2012) Effect of friction stir welding on microstructure, mechanical and wear properties of AA6061/ZrB₂ in situ cast composites. *Mater Sci Eng A* 543:257–266

8. Dixit US, Pandey PM, Verma GC (2019) Ultrasonic-assisted machining processes: a review. *Int J Mechatron Manufact Syst* 12(3–4):227–254
9. Firouzdor V, Kou S (2010) Formation of liquid and intermetallics in Al-to-Mg friction stir welding. *Metall Mater Trans A* 41(12):3238–3251
10. Firouzdor V, Kou S (2010) Al-to-Mg friction stir welding: effect of material position, travel speed, and rotation speed. *Metall Mater Trans A* 41(11):2914–2935
11. Foster DR, Dapino MJ, Babu SS (2013) Elastic constants of ultrasonic additive manufactured Al 3003–H18. *Ultrasonics* 53:211–218
12. Friel RJ (2015) Power ultrasonics for additive manufacturing and consolidating of materials. In: *Power ultrasonics: applications of high-intensity ultrasound*, pp 313–35
13. Friel RJ, Harris RA (2010) A nanometre-scale fibre-to-matrix interface characterization of an ultrasonically consolidated metal matrix composite. *Proceed Inst Mech Eng Part L: J Mater: Des Appl* 224(1):31–40
14. Friel RJ, Harris RA (2013) Ultrasonic additive manufacturing a hybrid production process for novel functional products. *Procedia CIRP* 6(1):35–40
15. Gibson I, Rosen DW, Stucker B (2010) Sheet lamination processes. In: *Additive manufacturing technologies*, pp 223–52
16. Hahnen R, Dapino MJ (2014) NiTi–Al interface strength in ultrasonic additive manufacturing composites. *Compos B Eng* 59:101–108
17. Hehr A, Dapino MJ (2015) Interfacial shear strength estimates of NiTi–Al matrix composites fabricated via ultrasonic additive manufacturing. *Compos B Eng* 77:199–208
18. Hopkins CD, Wolcott PJ, Dapino MJ, Truog AG, Babu SS, Fernandez SA (2012) Optimizing ultrasonic additive manufactured Al 3003 properties with statistical modeling. *J Eng Mater Technol Trans ASME* 134:011004
19. Johnson K Ultrasonic consolidation—A viable method of smart structure manufacture. In: *4th International conference on rapid manufacturing*
20. Kar A, Yadav D, Suwas S, Kailas SV (2020) Role of plastic deformation mechanisms during the microstructural evolution and intermetallics formation in dissimilar friction stir weld. *Mater Character* 164:110371
21. Kishor B, Chaudhari GP, Nath SK (2014) Cavitation erosion of thermomechanically processed 13/4 martensitic stainless steel. *Wear* 319:150–159
22. Kong C, Soar RC, Dickens PM (2004) Optimum process parameters for ultrasonic consolidation of 3003 aluminium. *J Mater Process* 146(2):181–187
23. Kong CY, Soar R (2005) Method for embedding optical fibers in an aluminum matrix by ultrasonic consolidation. *Appl Opt* 30:6325–6333
24. Kumar S (2016) Ultrasonic assisted friction stir processing of 6063 aluminum alloy. *Archiv Civil Mech Eng* 16(3):473–484
25. Kumar S, Wu CS, Padhy GK, Ding W (2017) Application of ultrasonic vibrations in welding and metal processing: a status review. *J Manuf Process* 26:295–322
26. Kumar S, Wu CS (2017b) Ultrasonic vibrations in friction stir welding: state of the art. In: *7th International conference on welding science and engineering (WSE 2017) in conjunction with 3rd international symposium on computer-aided welding engineering (CAWE 2017)*
27. Kumar S, Ding W, Sun Z, Wu CS (2018) Analysis of the dynamic performance of a complex ultrasonic horn for application in friction stir welding. *Int J Adv Manuf Technol* 97(1–4):1269–1284
28. Kumar S, Wu CS, Zhen S, Ding W (2019) Effect of ultrasonic vibration on welding load, macrostructure, and mechanical properties of Al/Mg alloy joints fabricated by friction stir lap welding. *Int J Adv Manuf Technol* 100(5–8):1787–1799
29. Kumar S, Wu C, Gao S (2020) Process parametric dependency of axial downward force and macro- and microstructural morphologies in ultrasonically assisted friction stir welding of Al/Mg alloys. *Metall Mater Trans A* 51:2863–2881
30. Kumar S, Wu C, Shi L (2020) Intermetallic diminution during friction stir welding of dissimilar Al/Mg alloys in lap configuration via ultrasonic assistance. *Metall Mater Trans A* 51:5725–5742

31. Kumar S, Wu CS (2017) Review: Mg and its alloy—Scope, future perspectives and recent advancements in welding and processing. *J Harbin Inst Technol* 24(06):1–37
32. Kumar S, Wu CS (2018) A novel technique to join Al and Mg alloys: ultrasonic vibration assisted linear friction stir welding. *Materials Today: Proc* 5(9):18142–18151
33. Kumar S, Wu CS (2020) Suppression of intermetallic reaction layer by ultrasonic assistance during friction stir welding of Al and Mg based alloys. *J Alloys Comps* 827:154343
34. Langenecker B (1966) Effects of ultrasound on deformation characteristics of metals. *Trans Sonics Ultrasonics* 13(1):1–8
35. Laugier P, Haiat G (2011) Introduction to the physics of ultrasound. In: *bone quantitative ultrasound*, pp 29–45
36. Lee K-J, Kwon E-P (2014) Microstructure of stir zone in dissimilar friction stir welds of AA6061-T6 and AZ31 alloy sheets. *Trans Nonfer Metals Soc China* 24(7):2374–2379
37. Levy A, Miriyev A, Sridharan N, Han T, Tuval E, Babu SS, Dapino MJ, Frage N (2018) Ultrasonic additive manufacturing of steel: method, post-processing treatments and properties *J Mater Process Technol* 256:183–189
38. Li J, Monaghan T, Masurtschak S, Bournias-Varotsis A, Friel RJ, Harris RA (2015) Exploring the mechanical strength of additively manufactured metal structures with embedded electrical materials. *Mater Sci Eng, A* 639:474–481
39. Li Y, Cheng Z, Chen X, Long Y, Li X, Li F, Li J, Twiefel J (2019) Constitutive modeling and deformation analysis for the ultrasonic-assisted incremental forming process. *Int J Adv Manuf Technol* 104:2287–2299
40. Liu XC, Wu C, Padhy GK (2015) Characterization of plastic deformation and material flow in ultrasonic vibration enhanced friction stir welding. *Scripta Mater* 102:95–98
41. Liu XC, Wu CS, Padhy GK (2015) Improved weld macrosection, microstructure and mechanical properties of 2024Al-T4 butt joints in ultrasonic vibration enhanced friction stir welding. *Sci Technol Weld Joining* 20(4):345–352
42. Liu XC, Wu CS (2016) Elimination of tunnel defect in ultrasonic vibration enhanced friction stir welding. *Mater Des* 90:350–358
43. Lv XQ, Wu C, Yang C, Padhy GK (2018) Weld microstructure and mechanical properties in ultrasonic enhanced friction stir welding of Al alloy to Mg Alloy. *J Mater Process Technol* 254:145–157
44. Ma H, He DQ, Liu JS (2015) Ultrasonically assisted friction stir welding of aluminium alloy 6061. *Sci Technol Welding Joining* 20(3):216–221
45. Mariani E, Ghassemieh E (2010) Microstructure evolution of 6061 O Al alloy during ultrasonic consolidation: an insight from electron backscatter diffraction. *Acta Mater* 58(7):2492–2503
46. Monaghan T, Capel AJ, Christie SD, Harris RA, Friel RJ (2015) Solid-state additive manufacturing for metallized optical fiber integration. *Compos A Appl Sci Manuf* 76:181–193
47. Mou C, Saffari P, Li D, Zhou K, Zhang L, Soar R, Bennion I (2009) Smart structure sensors based on embedded fibre bragg grating arrays in aluminium alloy matrix by ultrasonic consolidation. *Meas Sci Technol* 20:34013
48. Moustafa AR, Durga A, Lindwall G, Cordero ZC (2020). Scheil ternary projection (STeP) diagrams for designing additively manufactured functionally graded metals. *Additive Manuf* 32:101008
49. Ning F, Cong W (2020) Ultrasonic vibration-assisted (UV-A) manufacturing processes: state of the art and future perspectives. *J Manuf Process* 51:174–190
50. Obielodan J, Stucker B (2014) A fabrication methodology for dual-material engineering structures using ultrasonic additive manufacturing. *Int J Adv Manuf Technol* 70:277–284
51. Padhy GK, Wu CS, Gao S, Shi L (2016) Local microstructure evolution in Al 6061–T6 friction stir weld nugget enhanced by ultrasonic vibration. *Mater Des* 92:710–723
52. Pal D, Stucker B (2013) A study of subgrain formation in Al 3003 H-18 foils undergoing ultrasonic additive manufacturing using a dislocation density based crystal plasticity finite element framework. *J Appl Phys* 113:203517
53. Park K, Kim GY, Ni J (2007) Design and analysis of ultrasonic assisted friction stir welding. In: *ASME international mechanical engineering congress and exposition*, vol 3

54. Park K (2009) Development and analysis of ultrasonic assisted friction stir welding process. 125
55. Patel V, Li W, Xu Y (2018) Stationary shoulder tool in friction stir processing: a novel low heat input tooling system for magnesium alloy. In: *Materials and manufacturing processes*, pp 1–6
56. Printing metal 3D objects using sounds. (n.d.). Retrieved 10 Mar 2021 from <https://www.metaworkingworldmagazine.com/printing-metal-3d-objects-using-sounds/>
57. Ram G, Yang Y, Stucker BE (2006) Effect of process parameters on bond formation during ultrasonic consolidation of aluminum alloy 3003. *J Manuf Syst*
58. Ram GDJ, Robinson C, Yang Y, Stucker BE (2007) Use of ultrasonic consolidation for fabrication of multi-material structures. *Rapid Prototyping J* 13(4):226–235
59. Robinson CJ, Stucker B, Lopes AJ, Wicker R, Palmer JA (2006) Integration of Direct-Write (DW) and Ultrasonic Consolidation (UC) technologies to create advanced structures with embedded electrical circuitry. In: *17th Solid freeform fabrication symposium, SFF 2006*
60. Ruilin L, Diqiu H, Luocheng L, Shaoyong Y, Kunyu Y (2014) A study of the temperature field during ultrasonic-assisted friction-stir welding. *Int J Adv Manuf Technol* 73(1–4):321–327
61. Schomer JJ (2017). Embedding fiber bragg grating sensors through ultrasonic additive manufacturing
62. Schwoppe LA, Friel RJ, Johnson KE, Harris RA (2009) Field repair and replacement part fabrication of military components using ultrasonic consolidation cold metal deposition. In: *RTO-MP-AVT-163-additive technology for repair of military hardware*
63. Shi L, Wu CS, Liu XC (2015) Modelling the Effects of Ultrasonic Vibrations in Friction Stir Welding. *J Mater Process Technol* 222:91–102
64. Shimizu S, Fujii HT, Sato YS, Kokawa H, Sriraman MR, Babu SS (2014) Mechanism of weld formation during very-high-power ultrasonic additive manufacturing of Al Alloy 6061. *Acta Mater* 74:234–243
65. Siggard EJ, Madhusoodanan AS, Stucker B, Eames B (2006) Structurally embedded electrical systems using ultrasonic consolidation (UC). In: *17th solid freeform fabrication symposium, SFF 2006*
66. Singh S, Prakash C, Gupta MK (2020) On friction-stir welding of 3D printed thermoplastics. In: *Materials forming, machining and post processing*. Springer, pp 75–91
67. Sojiphan K, Sriraman MR, Babu SS (2010) Stability of microstructure in Al3003 builds made by very high power ultrasonic additive manufacturing. In: *21st Annual international solid freeform fabrication symposium—An additive manufacturing conference, SFF 2010*
68. Song X, Feih S, Zhai W, Sun CN, Li F, Maiti R, Wei J, Yang Y, Oancea V, Brandt LR, Korsunsky AM (2020). Advances in additive manufacturing process simulation: residual stresses and distortion predictions in complex metallic components. *Mater Des* 193:108779
69. Sridharan N, Norfolk M, Babu SS (2016) Characterization of steel-Ta dissimilar metal builds made using very high power ultrasonic additive manufacturing (VHP-UAM). *Metall Mater Trans A* 47(5):2517–2528
70. Sriraman M, Gonser M, Fujii HT, Babu SS, Bloss M (2011) Thermal transients during processing of materials by very high power ultrasonic additive manufacturing. *J Mater Process Technol* 211:1650–1657
71. Tarasov SY, Rubtsov VE, Fortuna SV, Eliseev AA, Chumaevsky AV, Kalashnikova TA, Kolubaev EA (2017) Ultrasonic-assisted aging in friction stir welding on Al–Cu–Li–Mg aluminum alloy. *Welding World* 61(4):679–690
72. Thomä M, Gester A, Wagner G, Straß B, Wolter B, Benfer S, Gowda DK, Fürbeth W (2019) Application of the hybrid process ultrasound enhanced friction stir welding on dissimilar aluminum/dual-phase steel and aluminum/magnesium joints. *Materialwiss Werkstofftech* 50(8):893–912
73. Ultrasound. (n.d.) Retrieved from <https://en.wikipedia.org/wiki/Ultrasound>
74. White D (2000) Ultrasonic object consolidation. US Patent 6,519,500
75. Wielage B, Hoyer I, Weis S (2007) Soldering aluminum matrix composites. *Welding J (Miami, Fla)* 86:67–70

76. Wolcott PJ, Hehr A, Dapino MJ (2014) Optimized welding parameters for Al 6061 ultrasonic additive manufactured structures. *J Mater Res* 29(17):2055–2065
77. Yadav VK, Gaur V, Singh IV (2020) Effect of post-weld heat treatment on mechanical properties and fatigue crack growth rate in welded AA-2024. *Mater Sci Eng A* 779:139116.
78. Yan J, Xu Z, Shi L, Ma X, Yang S (2011) Ultrasonic assisted fabrication of particle reinforced bonds joining aluminum metal matrix composites. *Mater Des* 32(1):343–347
79. Yang Y, Ram GJ, Stucker BE (2009) Bond formation and fiber embedment during ultrasonic consolidation. *J Mater Process Technol* 209(10):4915–4924
80. Zhao Y, Huang L, Zhao Z, Yan K (2016) Effect of travel speed on the microstructure of Al-to-Mg FSW joints. *Mater Sci Technol* 32(10):1025–1034
81. Zhong YB, Wu CS, Padhy GK (2017) Effect of ultrasonic vibration on welding load, temperature and material flow in friction stir welding. *J Mater Process Technol* 239:279–283